Accuracy Assessment of Structure from Motion Photogrammetry and LiDAR for Topographic Modeling and Change Detection

1. Introduction

Recent advancements in unoccupied aerial vehicles (UAVs) have revolutionized geomorphic surveys by enabling cost-effective and rapid acquisition of high-resolution topographic data. Structure from Motion (SfM) photogrammetry, in particular, has democratized 3D topographic modeling by generating dense point clouds at minimal expense (Smith, Carrivick and Quincey, 2016). However, challenges such as vegetation interference and shadow effects may compromise SfM accuracy, necessitating complementary technologies like airborne Light Detection and Ranging (LiDAR), which offers superior penetration capabilities (MacDonell *et al.*, 2023).

This study focuses on Swindale Beck, a dynamic fluvial system in Cumbria, UK (54°30′28″N, 2°45′18″W), characterized by mixed wet and dry terrain. The research aims to:

1) Evaluate the vertical accuracy differences between DSMs generated by SfM photogrammetry and LiDAR
2) Quantify sediment deposition and erosion using multi-temporal DEMs (2018, 2020, 2023).
3) Compare different error propagation models (Minimum LoD vs. Probabilistic Thresholding) in geomorphic change detection.

The report is structured as follows: Methods detail data acquisition and processing workflows; Results present accuracy metrics and topographic changes; Discussion contextualizes findings and limitations; and Conclusions summarize key outcomes.

2. Method

1) Study Area and Data Acquisition

The study area spans around 200 meters along Swindale Beck, with a channel width of 6–10 meters. Data collection included:

Year	Data Type	Processing Methods	Output
2018	DEM	Geomorphic Change Detection Analysis	Topographic Change Maps
2020	UAV SfM Bathymetric Data	Pix4D: DSM & Orthoimage; GNSS GCPs for accuracy assessment	DSM 2020 & Orthophoto

2023	UAV LiDAR Bathymetric Data	& wet DEM Ground Classification Generate wet DEM	DEM 2023

Table 1 Datasets and related information

The workflow of this project is shown belowDistribution map is shown in Figure 2:

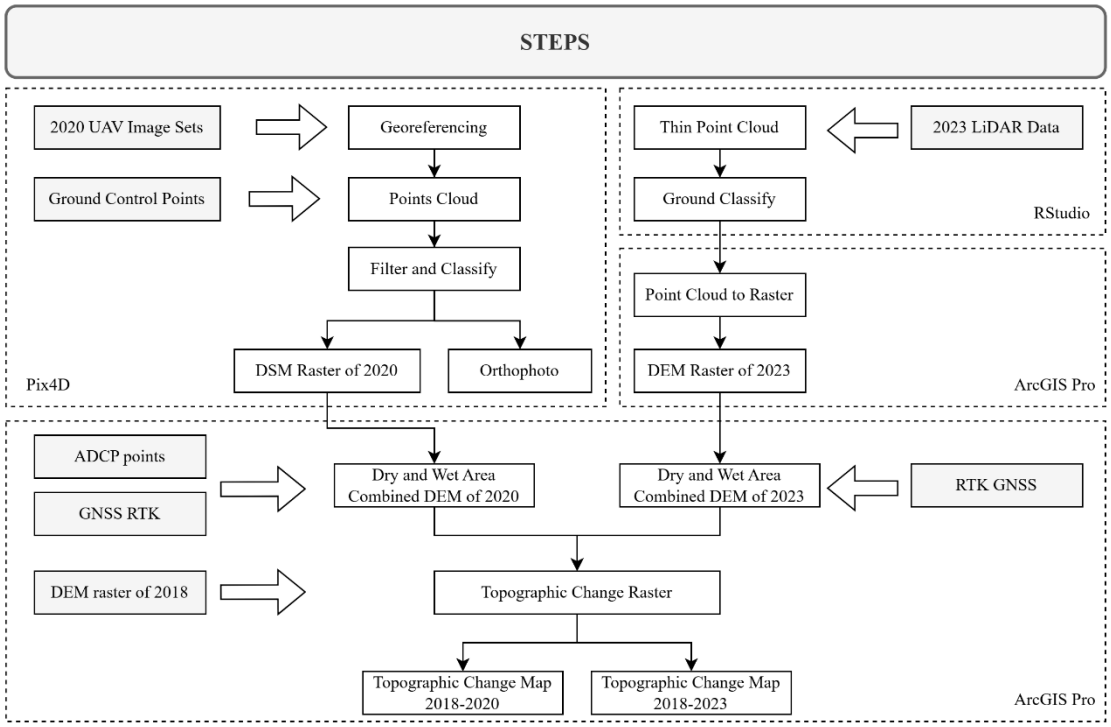

Figure 1 Data processing workflow

2) UAV SfM Data Processing (2020)

A DJI Phantom 4 RTK drone was used for aerial data collection with a Double Grid flight pattern and Oblique Photography. A total of 95 images were processed in Pix4D to generate DSM and orthophoto.

i. GCP Selection: Following the rule that ground control points should be scattered (Stott, Williams and Hoey, 2020), a combination of edge and center GCPs (A1, A2, A5, B1, B6, B8) was used to minimize systematic error. Five additional points (A3, A7, A8, B3, B7) served as independent checkpoints to assess model accuracy. The distribution map is shown in Figure 2.

ii. Accuracy Assessment: RMSE was computed by comparing GCP and checkpoint elevations with DSM (n=11).

$$RMSE = \sqrt{\frac{\sum_{i=1}^{n}\left(Z_{DEM,i} - Z_{GCP,i}\right)^2}{n}}$$

iii. DEM Alignment Verification: To ensure the reliability of the photogrammetric outputs, DEM alignment errors were quantified through two complementary approaches:

The Pix4D-generated RMSE (Root Mean Square Error) provides a comprehensive assessment of the photogrammetric workflow, incorporating uncertainties from image matching, camera calibration, and RTK georeferencing. This metric reflects the *internal consistency* of the SfM-derived DSM by comparing its elevations against ground control points (GCPs).

To validate the Pix4D results and address potential biases in proprietary software outputs, the Extract Values to Points tool in ArcGIS Pro was used to sample DSM elevations at all GCP and checkpoint locations.

3) LiDAR Data Processing (2023)
   i. Ground Classification: RStudio and the lidR package were used to filter ground points.
   ii. DEM Generation: The LiDAR point cloud was converted into a raster DEM and aligned with the 2020 SfM DSM using the Resample tool in ArcGIS Pro.
4) Topographic Change Detection

DEM differencing was performed using GCD (Geomorphic Change Detection) software. Errors are shown below:

Year	2018	2020	2023
Dry (m)	0.13	0.177	0.059
Wet (m)	0.12	0.10	0.10

Table 2 Error value

Uncertainty Analysis Methods:

i. Ground Classification: RStudio and the lidR package were used to filter ground points.
ii. Error Propagation.
iii. Probabilistic Thresholding (Constant 95%, Constant 68% and Variable 95%)

Variable 95% was selected as the most reliable method due to its ability to account for spatially variable errors in wet and dry regions.

3. Results

1) DSM Accuracy Assessment

	2020UAV			**2023LiDAR**
	Pix4D Quality Report		**Calculated**	
	GCP Error Z	**CP Error Z**	**GCP Error Z**	**GCP Error Z**
Mean [m]	0.021	0.050	0.042	
Sigma [m]	0.039	0.058	0.171	
RMS Error [m]	0.044	0.077	0.051	-0.041

*LiDAR error comes from(MacDonell *et al.*, 2023)

Table 3 DSM Error

LiDAR exhibited superior vertical accuracy (RMSE = 0.051 m) compared to SfM (RMSE = 0.077 m).

2) Orthophoto and GCP Distribution

A georeferenced orthophoto was generated in Pix4D and overlaid with GCP locations to assess spatial accuracy

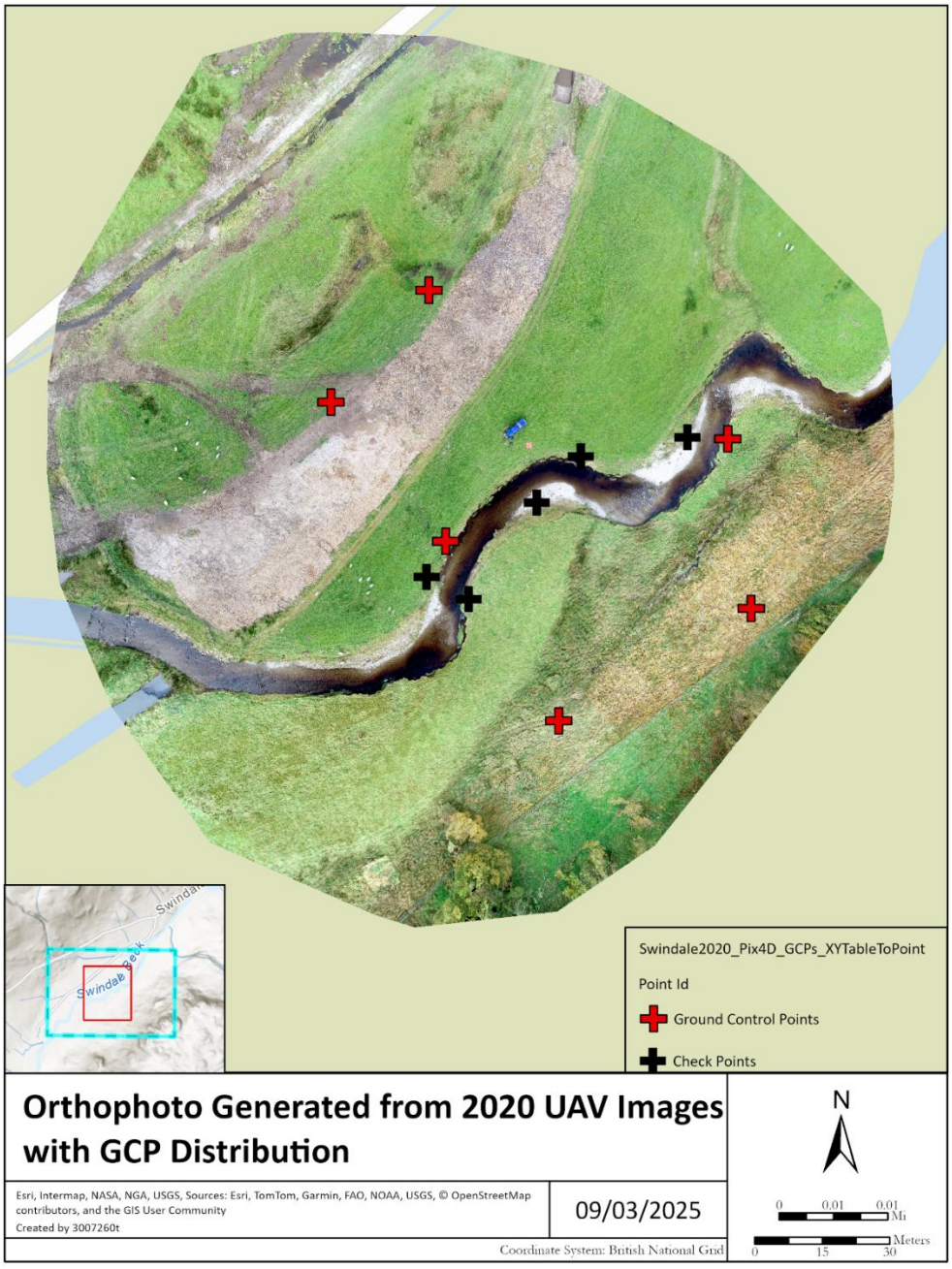

Figure 2 Orthophoto with GCPs distribution

3) DEMs based on Structure from Motion photogrammetry and LiDAR

The DEM generated by LiDAR is relatively smooth compared to SfM.

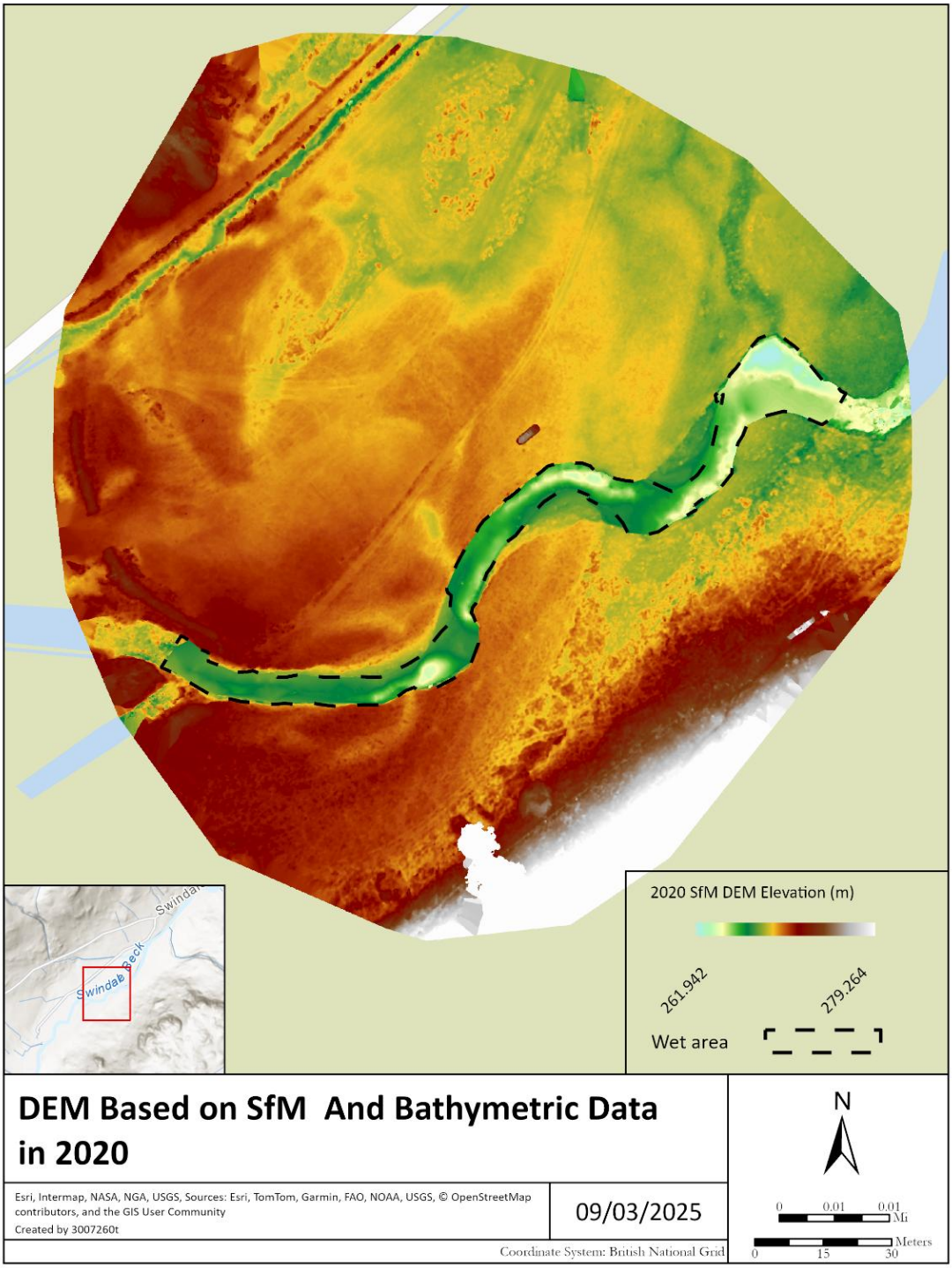

Figure 3 DEM based on SfM and bathymetric data in 2020

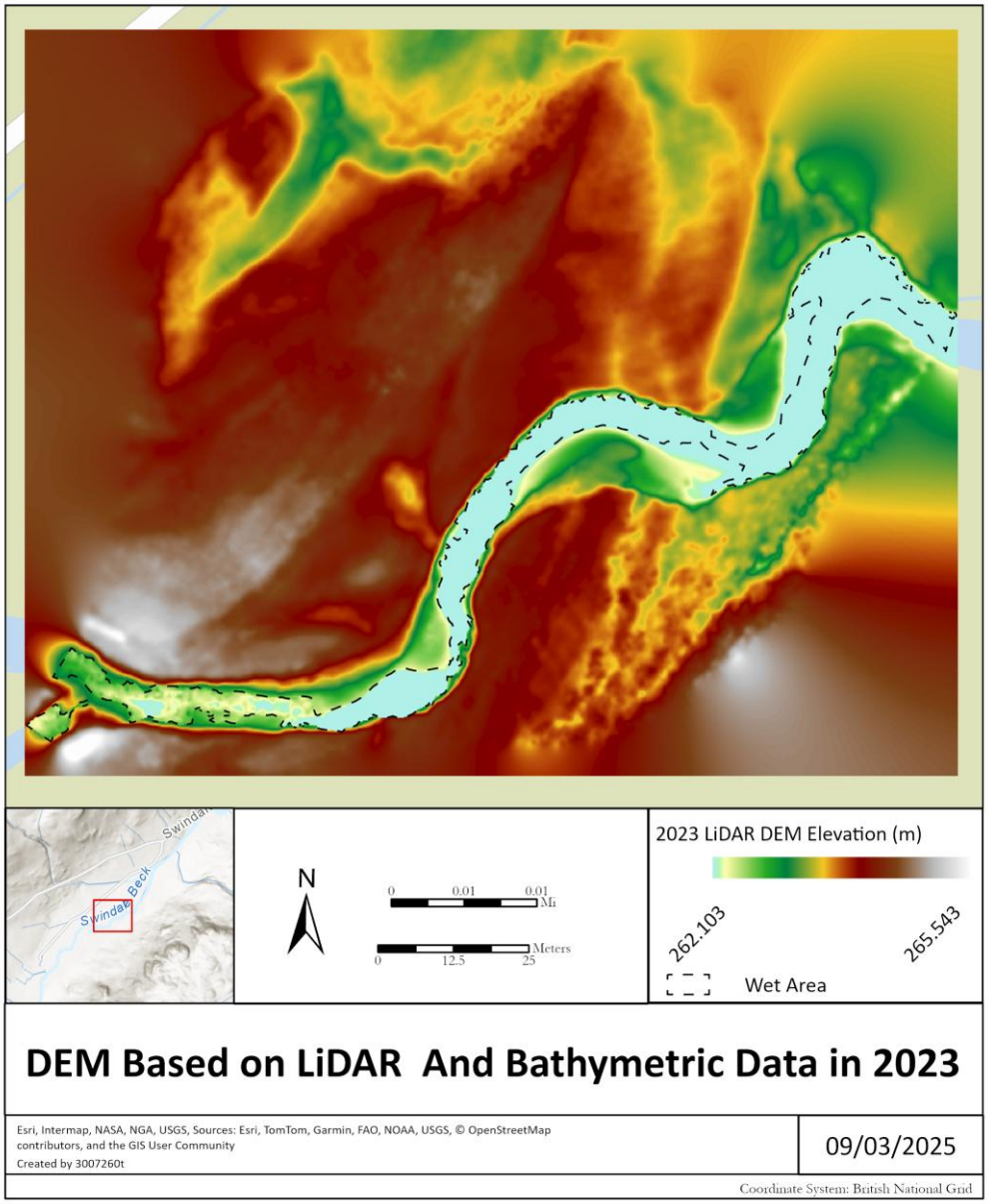

Figure 4 Figure 4 DEM based on LiDAR and bathymetric data in 2023

4) Topographic Change Quantification:

Probabilistic Thresholding (Variable 95%) outperformed Minimum LoD and propagated error by accounting for spatially heterogeneous errors in wet/dry zones. This method of calculating variation is therefore chosen. In order to quantify the topographic change, this part not only provides the topographic change map, but also calculates the volume of deposition/erosion, as shown in Table 4.

	2018-2020			2018-2023		
	Deposition [m³]	Erosion [m³]	Net Change [m³]	Deposition [m³]	Erosion [m³]	Net Change [m³]
Dry	26.71	283.77	-257.06	18.4	620.57	-602.18
Wet	64.04	15.48	48.56	113.74	40.44	73.31

Total	90.75	299.26	-208.51	132.14	661.01	-528.87

Table 4 Volumetric change metrics

Erosion dominated dry regions (e.g., -602.18 m³ net loss in 2018–2023), while wet areas showed deposition (+73.31 m³). The DEM of Difference (DoD) is shown below:

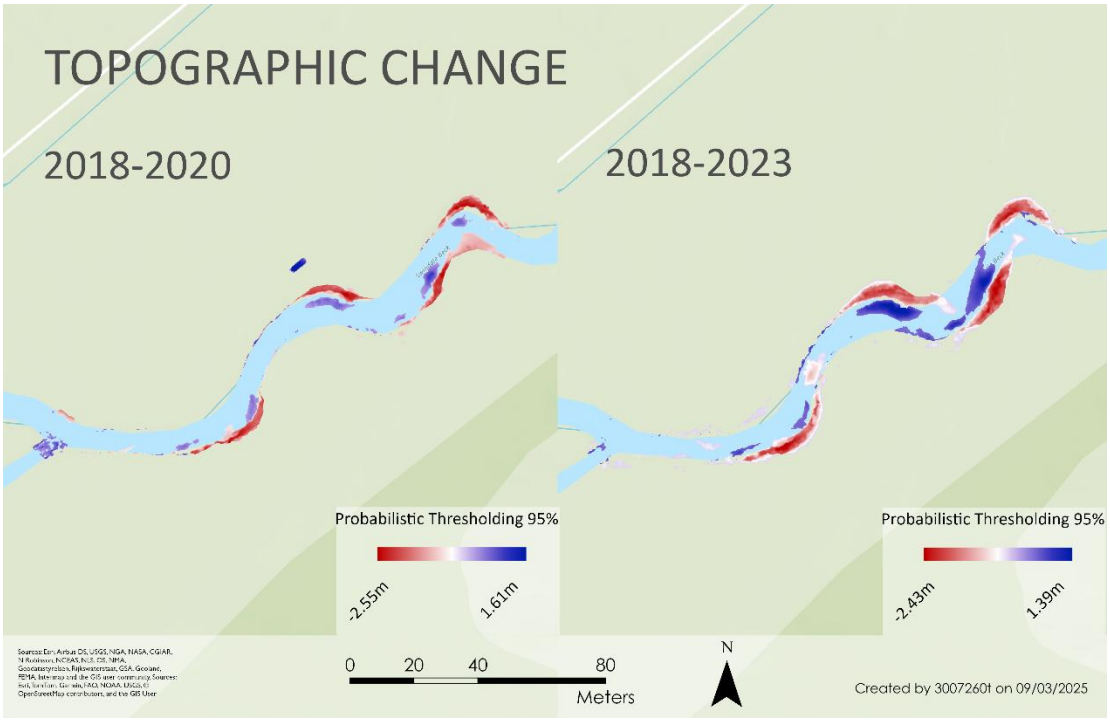

Figure 5 Topographic change map

Based on Figure 5, the spatial distribution of sediment deposition and erosion exhibits distinct patterns along the Swindale Beck channel. Deposition is mainly concentrated in the inner bends of meander sections, where reduced flow velocity facilitates sediment accumulation. In contrast, significant erosion is observed along the outer bends and steep banks, particularly in the upstream and midstream sections. In addition, localized erosion hotspots can be seen in narrower sections of the channel. These spatial patterns align with typical fluvial dynamics.

4. Discussion and Limitations

1) Comparison of SfM and LiDAR for DEM Generation
   The accuracy of SfM is not as good as that of LiDAR. For example, the error of SfM is 0.17m, while that of LiDAR is only 0.059m. It may be because of the influence of vegetation and shadows on the ground (MacDonell *et al.*, 2023), but it may also be because no other measures have been taken to eliminate the errors caused by surface feature.
2) Limitations and Future Recommendations
   i. Surface Cover Influence: The presence of gravel and vegetation introduced uncertainties in DSM generation, suggesting the need for

multispectral classification. Moreover, Sanz-Ablanedo et al. (2020) suggested that UAV SfM DEMs may have a systematic "doming" error due to camera geometry modelling limitations, that is, the entire DEM shows systematic upward deformation. This type of error is particularly noticeable in the area with relatively flat terrain. This error can be effectively reduced by optimising the route design, for example by adopting the Point of Interest (POI) aerial photography mode(Sanz-Ablanedo *et al.*, 2020).

ii. Flight Design Optimization: Additional datasets such as P4_singlegrid_centrelook could be incorporated to compare DEM outputs and refine modeling approaches.

iii. GCP Selection Sensitivity: Future work could explore different GCP combinations to identify the most optimal configurations.

5. Conclusion

LiDAR DEM demonstrated superior accuracy compared to UAV SfM. SfM errors primarily stemmed from image matching and GCP distribution. Topographic change trends indicate deposition from 2018-2020, ranging from 0 to 2.7 m (2018-2023), concentrated in the inner bends, while erosion increased from 0-0.9 m (2018-2020) to 0-1.2 m (2018-2023). DEM uncertainties were assessed separately for dry and wet regions, and probabilistic thresholding (Variable 95%) was the most effective method for filtering false change signals.

6. References

MacDonell, C.J. *et al.* (2023) 'Consumer-grade UAV solid-state LiDAR accurately quantifies topography in a vegetated fluvial environment', *Earth Surface Processes and Landforms*, 48(11), pp. 2211–2229. Available at: https://doi.org/10.1002/esp.5608.

Sanz-Ablanedo, E. *et al.* (2020) 'Reducing systematic dome errors in digital elevation models through better UAV flight design', *Earth Surface Processes and Landforms*, 45(9), pp. 2134–2147. Available at: https://doi.org/10.1002/esp.4871.

Smith, M.W., Carrivick, J.L. and Quincey, D.J. (2016) 'Structure from motion photogrammetry in physical geography', *Progress in Physical Geography: Earth and Environment*, 40(2), pp. 247–275. Available at: https://doi.org/10.1177/0309133315615805.

Stott, E., Williams, R.D. and Hoey, T.B. (2020) 'Ground Control Point Distribution for Accurate Kilometre-Scale Topographic Mapping Using an RTK-GNSS Unmanned Aerial Vehicle and SfM Photogrammetry', *Drones*, 4(3), p. 55. Available at: https://doi.org/10.3390/drones4030055.